

This article was downloaded by: [University of Haifa Library]

On: 13 August 2012, At: 20:31

Publisher: Taylor & Francis

Informa Ltd Registered in England and Wales Registered Number: 1072954 Registered office: Mortimer House, 37-41 Mortimer Street, London W1T 3JH, UK



## Molecular Crystals and Liquid Crystals

Publication details, including instructions for authors and subscription information:

<http://www.tandfonline.com/loi/gmcl20>

## Nonlinear Optical Spectroscopy of Porphyrins and Mesoionic Compounds

Cid B. De Araújo<sup>a</sup>, A. S. L. Gomes<sup>a</sup> & I. E. Borissevitch<sup>a</sup>

<sup>a</sup> Departamento de Física, Universidade Federal de Pernambuco, Recife, PE, 50670-901, Brazil

Version of record first published: 29 Oct 2010

To cite this article: Cid B. De Araújo, A. S. L. Gomes & I. E. Borissevitch (2002): Nonlinear Optical Spectroscopy of Porphyrins and Mesoionic Compounds, *Molecular Crystals and Liquid Crystals*, 374:1, 357-366

To link to this article: <http://dx.doi.org/10.1080/713738249>

PLEASE SCROLL DOWN FOR ARTICLE

Full terms and conditions of use: <http://www.tandfonline.com/page/terms-and-conditions>

This article may be used for research, teaching, and private study purposes. Any substantial or systematic reproduction, redistribution, reselling, loan, sub-licensing, systematic supply, or distribution in any form to anyone is expressly forbidden.

The publisher does not give any warranty express or implied or make any representation that the contents will be complete or accurate or up to date. The accuracy of any instructions, formulae, and drug doses should be independently verified with primary sources. The publisher shall not be liable for any loss, actions, claims, proceedings, demand, or costs or damages whatsoever or howsoever caused arising directly or indirectly in connection with or arising out of the use of this material.



## Nonlinear Optical Spectroscopy of Porphyrins and Mesoionic Compounds

CID B. DE ARAÚJO, A. S. L. GOMES and  
I. E. BORISSEVITCH\*

*Departamento de Física, Universidade Federal de Pernambuco,  
50670-901 Recife, PE, Brazil*

*\*Present address: Departamento de Física e Matemática, Faculdade de  
Filosofia, Ciências e Letras de Ribeirão Preto, Universidade de São Paulo,  
14040-901 Ribeirão Preto, SP, Brazil*

We report on the third-order nonlinear optical properties of porphyrins derivatives (PPh) and mesoionic compounds (MIC). The role played by the chemical environment of PPh was investigated and a detailed interpretation is given for the results. Two-photon absorption in MIC was studied and the absorption cross-section was measured in the visible and in the near-infrared.

**Key words :** Nonlinear Optics, Biomaterials, Photonic Materials

### 1. INTRODUCTION

Nonlinear (NL) organic materials have been intensively studied in recent years [1-3]. The delocalization of  $\pi$  - electrons over molecular chains originate large nonlinearities and then light induced changes in the absorption coefficient and in the refractive index are easily observed in organic materials. Their applicability ranges from all-optical switches [4] to biomedical applications [5]. Effects such as NL refraction and two-photon absorption (TPA) are among the effects widely exploited for photonics applications of organics.

In this paper, we describe NL properties of two classes of materials: porphyrins derivatives and mesoionic compounds.

Most of the material presented here we learned from collaborative work and stimulated discussions with our colleagues and graduate

students. Thus, we would like to thank all of them and particularly to A. G. Bezerra Jr., N. Rakov, M. T. Oliveira, M. Trsic and A. M. Simas.

## 2. NONLINEAR REFRACTIVE EFFECTS IN PORPHYRINS

Porphyrins (PPh) are compounds with many biological representatives, such as hemes and chlorophylls. When doped with iron, PPh complexes, are important components of Nature, involved in various biological processes. Some PPh and their complexes with magnetic metals, in particular with Fe(III), may accumulate in tumors and can be used as contrast agents in tomography; applications in photodynamic therapy are already known.

Recently we reported measurements of the NL refractive index,  $n_2$ , of two water soluble PPh, a negatively charged meso-tetrakis (p-sulfonatophenyl) PPh, TPPS<sub>4</sub>, and a positively charged meso-tetrakis (4-N-methyl-pyridiniumyl) PPh, TMPyP, in their free-base forms and their Fe(III) and Mn(III) complexes [6]. Their structures are shown in Fig. 1.

TPPS<sub>4</sub> and TMPyP and their Fe(III) and Mn(III) complexes were obtained from Midcentury Chemicals and used as purchased. The compounds were dissolved in Milli-Q quality water and the concentration was controlled spectrophotometrically. The pH changes were produced by addition of HCl or NaOH stock solutions. The absorption coefficient of the samples at 532 nm was kept at  $\sim 2\text{cm}^{-1}$  adjusting the PPh concentration.

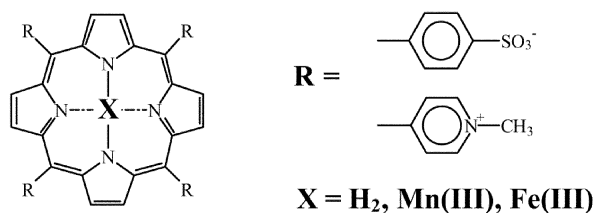


FIGURE 1 - Molecular structures of the PPh studied.

For measurements of  $n_2$  using the Z-scan technique [7], the second harmonic of a Q-switched and mode-locked Nd:YAG laser delivering pulses of 70 ps (FWHM) at 532 nm was used. A single pulse at 10 Hz rate was selected using a "pulse picker". The beam was focused in the sample which was mounted in a translation stage. A boxcar integrator was used to record the signals.

Time resolved experiments using the Kerr Gate technique [8] were also performed. The beam at 532 nm was split in two, a strong and a weak probe beam. Two crossed polarizers were introduced in the path of the probe beam, whereas the polarization of the strong beam was set at  $45^\circ$  with respect to the probe beam input polarization. A slow response detector connected to the boxcar obtained the data as a function of delay time between the strong and the weak pulses.

Fig. 2 shows the normalized transmittance as a function of the sample position when the small aperture Z-scan was used. The Z ordinate is measured along the beam direction, and  $Z < 0$  corresponds to locations between the focusing lens and its focal plane. The  $n_2$  value was obtained using the relation  $n_2 = \Delta T / (0.406 k L_{\text{eff}} I)$ , where  $I$  is the excitation intensity,  $k = 2\pi / \lambda$ ,  $L_{\text{eff}} = 1 - \exp(-\alpha L)$ ,  $\alpha$  is the linear absorption coefficient,  $\lambda = 532$  nm and  $L$  is the sample length [7].  $\Delta T$  is the difference between the peak and the valley transmittances in Fig.2.

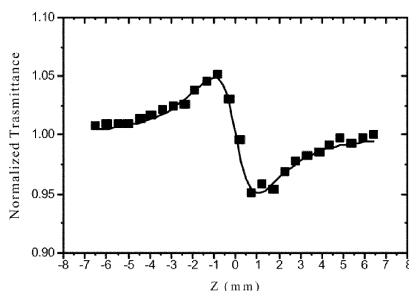


FIGURE 2 - Typical small-aperture Z-scan profile for PPh showing a self-defocusing nonlinearity.

Measurable values of  $n_2$  were observed for Fe(III)TMPyP, Mn(III)TMPyP and Mn(III)TPPS<sub>4</sub>. For the free base PPh forms and for Fe(III)TPPS<sub>4</sub> the values of  $n_2$  were below the sensitivity of the set up. The results are summarized in Table I. In general,  $n_2$  can be due to several mechanisms including the electronic polarizability and molecular reorientation. Normally the electronic contribution for  $n_2$  is enhanced when the wavelength of excitation is in resonance with an absorption band. However no relevant correlation between linear absorption and the  $n_2$  value was observed in the experiments.

Fig. 3 shows the absorption spectra of the PPh with the Soret band in the range 400nm - 500nm. Notice that the absorption at 532 nm for Mn(III)TMPyP, which has the largest  $n_2$  value, is lower than that for

Mn(III)TPPS<sub>4</sub> which has the  $n_2$  value 18 times lower. Moreover, the position of the Soret band for Mn(III)TPPS<sub>4</sub> is closer to the excitation

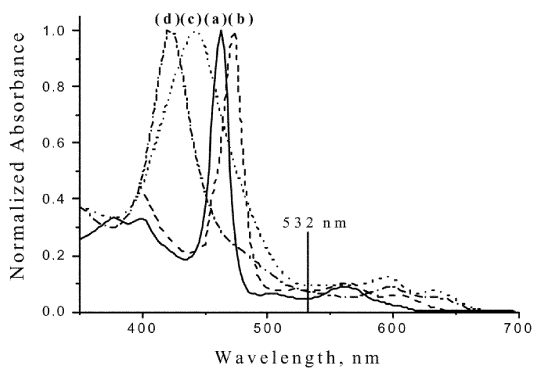


FIGURE 3 - Absorption spectra: (a) Mn(III)TMPyP, pH 7.0; (b) Mn(III)TPPS<sub>4</sub>, pH 7.0; (c) Fe(III)TMPyP, pH 4.0; and (d) Fe(III)TMPyP, pH 9.0.

**TABLE I** Nonlinear refractive index,  $n_2$ , at 532 nm.

PORPHYR		$n_2$ ( $10^{-14} \text{ cm}^2$ )
TMPyP		< -0.1
Fe(III)TMP		-0.6
Fe(III)TMP		-0.2
Fe(III)TMP		-0.1
Fe(III)TMP		-0.4
Mn(III)TM		-5.4
TPPS <sub>4</sub>		< -0.1
TPPS <sub>4</sub>		< -0.1
Fe(III)TPP		< -0.1
Fe(III)TPP		< -0.1
Mn(III)TPF		-0.3

wavelength than for Mn(III)TMPyP. Hence, the contribution of the electronic resonance to the observed signal is small and masked by

other mechanisms. The possibility of thermal effects was discarded due to the low repetition rate of the picosecond pulses.

Fig. 4 shows the Kerr Gate signal as a function of delay time [9]. The signal profile for the nonmetal PPh is symmetric and presents rise (and decay) time of  $\sim 18$  ps, whilst the Mn(III)PPh derivative presents a rise time of  $\sim 12$  ps and a two component signal with decay times of  $\sim 12$  ps and  $\sim 90$  ps. The fast component is in a time range of electronic and nuclear contributions while the decay time of 90 ps is characteristic of a orientational nonlinearity [1].

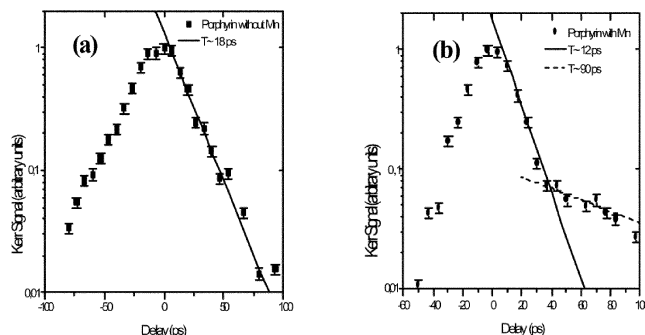


FIGURE 4 - Optical Kerr Gate signal as a function of delay time for (a) free base PPh and (b) PPh with Mn as the central atom in the ring plane.

Since both PPh are symmetric with respect to the plane of the  $\pi$ -conjugated ring the molecules have no electric dipole moment (EDM). However, the introduction of a central metal in the PPh may originate an EDM normal to the ring plane. To understand the origin of this EDM consider the following: (i) The central nitrogen atoms in free base PPh can be protonated, the  $pK_a$  value depending on the PPh structure. The  $TPPS_4$  molecule, with total negative charge, has two very close protonation  $pK_a$  values near pH 5.2. Above this pH value  $TPPS_4$  exists in a nonprotonated state as  $H_2TPPS_4$ ; below pH 5.2 formation of biprotonated  $(H^+)_2 H_2TPPS_4$  species is detected. The positively charged TMPyP molecule exists in aqueous solutions as deprotonated  $H_2TMPyP$  in the pH range from 0.9 to 12. The corresponding structures are symmetric with respect to the ring plane and hence these PPh have no EDM. This explains why  $n_2$  is negligible in any state of protonation. (ii) A permanent EDM perpendicular to the ring plane appears for PPh complexes with metals if the central metal atom comes out of the plane. Calculations show that the repulsion between the positively charged substituents ( $PPh(4^+)$ ) and the metal atom in the PPh

complexes increases the distance of the metal atom from the PPh ring and thus increases the dipole moment, while for negatively charged substituents (PPh(4-)) their attraction to the metal atom should decrease the EDM. The out of plane shift of the metal atom in the point charge model is negligible but, when axial ligands are present, the shift is considerably enhanced resulting in the increase of the EDM in the perpendicular direction to the ring plane. Thus, larger  $n_2$  values are expected for the PPh with metals.

In the Mn(III)PPh complexes in air-saturated solutions the metal atom is out of the plane of the PPh ring due to the binding of an oxygen molecule to Mn(III). This produces a dipole moment pointing from the ring to the Mn(III). The repulsion between Mn(III) and positively charged substituents in Mn(III)TMPyP increases this effect while the attraction between Mn(III) and negative substituents in Mn(III)TPPS<sub>4</sub> decreases it. This should explain the larger value of  $n_2$  for Mn(III)TMPyP as compared with that for Mn(III)TPPS<sub>4</sub>.

The Fe(III)PPh complexes in aqueous solutions present various monomeric species in equilibrium for different pH values as well as  $\mu$ -oxo-dimers  $\text{H}_2\text{O}-\text{Fe(III)PPh}-\text{O}-\text{Fe(III)PPh}-\text{H}_2\text{O}$ . At low pH, Fe(III)TPPS<sub>4</sub> assumes the form  $\text{H}_2\text{O}-\text{Fe(III)TPPS}_4-\text{OH}_2$ . Due to the attraction between Fe(III) and negatively charged substituents and simultaneous binding of two H<sub>2</sub>O molecules in symmetrical positions, the out-of-plane shift of Fe(III) is negligible. Thus the EDM is very small, and hence the  $n_2$  value as well. The highly symmetric structure of the  $\mu$ -oxo-dimer of Fe(III)TPPS<sub>4</sub> prevents the formation of an EDM and hence  $n_2$  is negligible. At higher pH, the Fe(III)TPPS<sub>4</sub> species form  $\mu$ -oxo-dimers via a sequence of reactions which are characterized by a single  $\text{pK}_a$  value ( $\cong 7.8$ ). Above this point Fe(III)TPPS<sub>4</sub> exists mainly as the  $\mu$ -oxo-dimer.

For Fe(III)TMPyP the equilibria of different forms is complex and two characteristic  $\text{pK}_a$  points are observed. According to the linear absorption, EPR and Z-scan data, below pH 4.7 (first  $\text{pK}_a$ ) there is an equilibrium between the symmetric species  $\text{H}_2\text{O}-\text{Fe(III)PPh}-\text{OH}_2$  and the nonsymmetric species  $\text{H}_2\text{O}-\text{Fe(III)PPh}$ . The electrostatic repulsion between the substituents and the Fe(III) atom induces the shift of the metal atom out of the plane of the PPh ring and produces an EDM even for  $\text{H}_2\text{O}-\text{Fe(III)PPh}-\text{OH}_2$ . The effect is more pronounced for the nonsymmetric form. Therefore the value of  $n_2$  at pH 4.0 is relatively high (Table I). The decrease of  $n_2$  at pH 7.0 is attributed to the absence of the  $\text{H}_2\text{O}-\text{Fe(III)PPh}$  species due to the formation of the  $\mu$ -oxo-dimer of Fe(III)TMPyP which is completely symmetric.

The small  $n_2$  observed at pH 9.0 as compared with that at pH 7.0 may be explained by the absence of the non-dimerized form  $\text{H}_2\text{O}-\text{Fe(III)TMPyP}-\text{H}_2\text{O}$  in favor of the  $\mu$ -oxo-dimer. At pH 11.5 the dimers should dissociate in favor of the  $\text{HO}^--\text{Fe(III)PPh}-\text{OH}^-$  form, thus increasing the EDM and the  $n_2$  value.

### 3. TWO-PHOTON ABSORPTION IN MESOIONIC COMPOUNDS

Amongst the existing materials, mesoionic compounds (MIC) were recently proposed as candidates for NL optics applications [10]. They are planar heterocyclic dipolar structures in which positive and negative charges are separated and delocalized within the  $\pi$  - electron system resulting dipole moments of  $\approx 5$  D.

The NL properties of a variety of MIC was investigated at 532 nm. The second hyperpolarizability was found to vary from  $0.8 \times 10^{-32}$  esu to  $1.5 \times 10^{-30}$  esu [11] while the TPA coefficient,  $\alpha_2$ , varied from 0.01 to 14 cm/GW [11]. Strong reverse saturable absorption leading to  $\approx 50\%$  reduction of the material's transmittance was observed [12]. Refs. [11, 12] illustrate some appropriate characteristics of MIC for NL optics applications. Particularly, we note the large potential of MIC for optical limiting at 532 nm. More recently we investigated the TPA process in MIC in the visible and in the near-infrared [13]. The results allowed to determine  $\alpha_2$  and the TPA cross-section ( $\sigma_{\text{TPA}}$ ).

The structures of the molecules studied are presented in Fig. 5. The synthesis of both compounds, Mesoionic-3-phenyl-5-aryl-4-methyl-1,4-thiazolium-2-thiolates (aryl = p-chlorophenyl, MIC-1, and phenyl, MIC-2), was described in ref. [12]. The samples consisted of liquid solutions of MIC dissolved in DMSO.

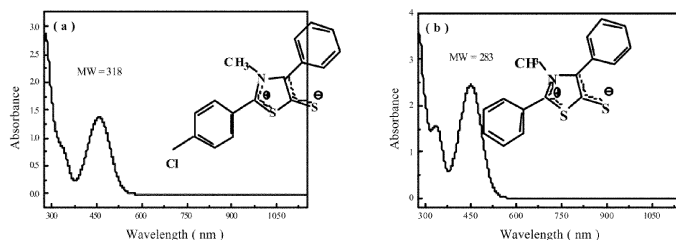


FIGURE 5 - Absorption spectra of the mesoionic compounds. The insets show the structure of the molecules and their molecular weight (MW). Length of the sample cell: 2 mm. (a) MIC-1; (b) MIC-2.



The absorption spectra of the samples are shown in Fig. 5. A transparency window from  $\approx 1120$  nm to  $\approx 550$  nm is observed. From 550 nm to 280 nm the spectra are characterized by absorption bands which correspond to transitions in the mesoionic molecules. The positions of the bands do not change with the samples' concentration in the range from 0.6 mg/ml to 1.4 mg/ml.

A Q-switched Nd: YAG laser (10 ns) and a dye laser pumped by the second harmonic of the laser were used. For the transmittance measurements the laser beam was split in two beams; one beam was used to monitor the energy of the incident pulses and the other was focused into the sample cell. The energy of the pulses transmitted through the sample was measured as a function of the incident intensity.

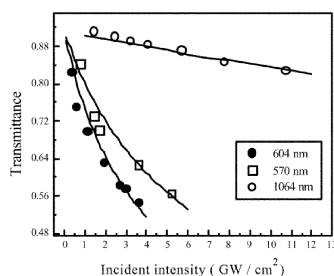


FIGURE 6 - Transmittance of MIC-1 (0.60 mg/ml) as a function of the laser intensity. The solid lines were obtained from the expression given in the text using the values of  $\alpha_1$  and  $\alpha_2$  shown in Table 1.

Fig. 6 illustrates the transmittance behavior of MIC-1 at 1064 nm, 604 nm and 570 nm, as a function of the laser intensity. Since one-photon absorption is not relevant at the wavelengths used, the changes in the transmittance are attributed to TPA because of the resonance between twice the laser frequencies and the absorption bands. This assumption is corroborated by the observation of fluorescence emission in the blue. The log-log plot of the blue fluorescence intensity versus the laser intensity gives a straight line with an almost quadratic slope.

A linear dependence of the signals intensity as a function of the MIC concentration was observed in the linear absorption, transmittance and fluorescence experiments.

The transmittance behavior is described through the equation  $dI(z)/dz = -\alpha_1 I(z) - \alpha_2 I^2(z)$ , where  $I(z)$  represents the beam intensity inside the medium and  $\alpha_1$  is the linear absorption coefficient. Upon integration, assuming that the beam has a Gaussian spatial profile and a rectangular temporal profile, we obtain for the transmittance of

energy the expression  $T = \exp(-\alpha_1 L)(1-R)^2 I_C I_0^{-1} \ln(1 + I_0/I_C)$ , where  $I_C = \alpha_1 / \alpha_2 (1-R) [1 - \exp(-\alpha_1 L)]$ ,  $I_0$  is the intensity in the front surface of the sample,  $R = 0.04$  is the reflectivity and  $L = 1$  cm is the sample thickness. The solid line in Fig.6 represents the fitting of the above expression for  $T$  using the parameters shown in Table II. The values of  $\sigma_{\text{TPA}}$  at 570 nm and 604 nm are larger than for 1064 nm probably because of the smaller detuning between the photon energies and the  $S_0 - S_1$  gap. However at 1064 nm the values of  $\sigma_{\text{TPA}}$  are larger than for rhodamines and fluorescein [13]. For 604 nm and 570 nm the values for MIC samples are of the same order of magnitude as for fluorescein [13]. Considering the small size of the mesoionic molecules, the possibility of making films of large density with a considerable TPA coefficient is an interesting challenge.

**TABLE II:** Parameters used to fit the transmittance data.  $\alpha_1$  was obtained from the linear absorption spectrum.

Sample	Concentration (mg/ml)	$\alpha_1$ (cm <sup>-1</sup> )	$\alpha_2$ (cm/GW)	$\sigma_{\text{TPA}}$ (cm <sup>4</sup> /GW)
MIC	0.60	0.01 @1064 nm 0.49 @604 nm 0.30 @570 nm	0.88 x 10 <sup>-20</sup> @1064 nm 0.43 x 10 <sup>-18</sup> @604 nm 0.26 x 10 <sup>-18</sup> @570 nm	
MIC	1.41	0.01 @1064 nm 0.20 @604 nm 0.23 @570 nm	0.33 x 10 <sup>-20</sup> @1064 nm 0.67 x 10 <sup>-19</sup> @604 nm 0.77 x 10 <sup>-19</sup> @570 nm	

#### 4. CONCLUSIONS

In this work we described NL refractive index measurements for porphyrins derivatives in the picosecond regime. It was shown how the environment (pH) affects the nonlinearity which is mainly due to a reorientational mechanism. We also described TPA in two novel mesoionic compounds, which present relatively high nonlinearities. The classes of materials discussed here are relevant for several applications, and is part of our research program in nonlinear optical materials.

#### ACKNOWLEDGEMENTS

We acknowledge financial support by the Brazilian Conselho Nacional de Desenvolvimento Científico e Tecnológico - CNPq.

## REFERENCES

- [1] P. N. Prasad and D. J. Williams, Introduction to Nonlinear Optical Effects in Molecules and Polymers (Wiley-Interscience, New York, 1991).
- [2] C. Bosshard, K. Sutter, P. Prêtre, J. Hulliger, M. Flörsheimer, P. Kaatz, and P. Günter, Organic Nonlinear Optical Materials (Gordon and Breach, Basel, 1995).
- [3] J. Zyss, ed., Molecular Nonlinear Optics (Academic Press, San Diego, 1994).
- [4] R. E. de Araujo, G. Borissevitch and A. S. L. Gomes, Electronics Letters, **36**, 71 (2000).
- [5] For a series of examples, see the issues of Biophotonics International, Laurin, also available on [www.Photonics.com](http://www.Photonics.com).
- [6] I. E. Borissevich, A. G. Bezerra Jr, A. S. L. Gomes, R. E. de Araujo, C. B. de Araújo, K. M. T. Oliveira, and M. Trisic, J. Porphyrin and Phtalocyanine, **5**, 51 (2001)
- [7] M. Sheik-Bahae, A. A. Said, T. H. Wei, D. J. Hagan, and E. W. Van Stryland, IEEE J. Quantum Electron., **QE-26**, 760 (1990).
- [8] P. P. Ho, in Semiconductors Probed by Ultrafast Laser Spectroscopy, Ed. R. R. Alfano (Academic Press, London, 1994), **vol. II**, pp 409.
- [9] A. G. Bezerra-Jr, I. E. Borissevitch, R. E. de Araujo, A. S. L. Gomes and C. B. de Araújo, Chem. Phys. Lett., **318**, 511 (1999).
- [10] G. L. C. Moura, A. M. Simas, and J. Miller, Chem. Phys. Lett., **257**, 639 (1996).
- [11] A. G. Bezerra-Jr, A. S. L. Gomes, P. F. Athayde-Filho, G. B. da Rocha, J. Miller and A. M. Simas, Chem. Phys. Lett., **309**, 421 (1999).
- [12] N. Rakov, C. B. de Araújo, G. B. da Rocha, A. M. Simas, P. A. F. Athayde-Filho, and J. Miller, Appl. Opt., **40**, 1389 (2000).
- [13] N. Rakov, C. B. de Araújo, G. B. da Rocha, A. M. Simas, P. A. F. Athayde-Filho, and J. Miller, Chem. Phys. Lett., **332**, 13 (2000).